Revue Roumaine de Chimie, **2008**, *53*(3), 217–221

TEM MICROGRAPHS FRACTAL ANALYSIS OF SILICA POWDERS

Gianina DOBRESCU,[a*] Emilia BALABANOVA,[b] Maria ZAHARESCU[a] and Niculae I. IONESCU[a]

[a]Institute of Physical Chemistry "Ilie .Murgulescu", Roumanian Academy, Spl.Independentei 202, 060021, Bucharest, Roumania
[b]Institute of Electronics – BAS, 72, Tzarigradsko chaussee blvd, 1784-Sofia, Bulgaria

Received February 28, 2007

TEM micrographs can be used to compute fractal dimensions of 3-dimensional objects. In order to covert the fractal dimension of TEM micrograph to the 3-dimensional fractal dimension, a modified sphere method was developed. Using this method, fractal dimensions of some nanosized silica powders were computed.

INTRODUCTION

Fractal theory was developed in the last two decades in order to achieve a better characterization of different phenomena in physics, chemistry, biology, medicine and so on.[1,2]

A direct method to determine fractal dimension is to analyze images obtained from scanning tunneling microscopy,[3-6] scanning probe microscopy,[7,8] transmission electron microscopy[9] (TEM). TEM micrographs can provide high-resolution pictures of 3-dimensional objects, such as ultrafine (nanosized) powders. Previously, fractal structural studies of silica aerogels were reported in literature.[10]

The aim of this paper is to analyzed TEM images and to obtain fractal dimensions of 3-dimensional objects, especially of some ultrafine silica powders. The powders are produced by thermal arc plasma method under the conditions of rapid cooling of silica vapour. The "mass-radius" relation is used to compute fractal dimension of TEM micrograph. The TEM micrograph fractal dimension is related to the 3-dimensional object (powder) fractal dimension. Some assumptions are to be made to obtain powder fractal dimension from TEM micrograph fractal dimension. These assumptions will be presented in chapter 2.

THEORY

Self-similarity, that is the main property of fractal objects, has a mathematical description:[1,2]

$$N(r/R) \sim (r/R)^{-D} \quad (1)$$

where D is fractal dimension and N(r, R) is the number of boxes of size r which cover the object of linear size R. Equation (1) leads to the following two methods for fractal dimension determination[11]. The "box counting" method,[12-14] when R is defined as the largest distance between any two points belonging to the system:

$$N_{box}(r) \sim r^{-D} \quad (2)$$

The "mass-radius" method:

$$N_{sites}(R) \sim R^{D} \quad (3)$$

where $N_{sites}(R)$ is the number of sites located within distance R from a given site, R>>r, (the mass in a sphere of radius R).

In this work the equation (3) is used to determine TEM micrographs fractal dimensions for R, varying in a broad range, from 1 pixel to the maximum radius of the cluster.

The image fractal dimension characterizes the plane object projection. Therefore, the fractal dimension of a 3-dimensional object will be bigger than TEM micrograph fractal dimension:

* Corresponding author: gdobrescu@icf.ro

$$D = D^{TEM} + D^{o} \quad (4)$$

where D is the powder fractal dimension, D^{TEM} is the image fractal dimension and D^{o} is a correction factor with fractal dimension behavior.

To compute the fractal dimension of a 3-dimensional object, the total number of r size boxes that covered the whole object must be measured. The number of r x r x r boxes, needed to covered the r x r x h parallelepiped (see Figure 1), will be $N_z(x_r, y_r, r)$, where x_r and y_r are center coordinates of parallelepiped xy-projection.

In this moment, the object fractal behavior along z axes is to be considered:

Fractal distribution along z axes

If, along z axes, 3-dimensional object exhibits a fractal behavior, it is easy to understand that the following relation can be written:

$$N_z(x_r, y_r, r) = A_z r^{-D_z} \quad (5)$$

where D_z is the fractal dimension along z-axes which means the exponent of scaling along z-axes. Equation (5) is obeyed even for r=1, and, therefore:

$$N_z(x_r, y_r, 1) = A_z(x_r, y_r) = \rho(x_r, y_r) \quad (6)$$

where $A(x_r,y_r)$ is a constant depending on chosen center x_r, y_r, and it is equal to the total sum of particles along z-axes described by coordinates x_r,y_r. This total sum of particles can be experimentally computed from grey-level of x_r,y_r pixel of TEM micrograph, $\rho(x_r,y_r)$. From equation (5) and (6) the following is obtained:

$$N_z(x_r, y_r, r) = \rho(x_r, y_r) r^{-D_z} \quad (7)$$

Total number of r size boxes needed to covered the whole object, N(r), can be computed as:

$$N(r) = \sum_{x_r, y_r} N_z(x_r, y_r, r) = r^{-D_z} \sum_{x_r, y_r} \rho(x_r, y_r) \quad (8)$$

Assuming that the grey level distribution has a fractal behavior so equation (1) is obeyed, we can write that the sum $\rho(x_r,y_r)$ scales with r like:

$$\theta(r) = \sum_{x_r, y_r} \rho(x_r, y_r) = B r^{-D_\theta} \quad (9)$$

Then, equation (8) becomes:

$$N(r) = B r^{-(D_z + D_\theta)} \quad (10)$$

It is obtained from equation (2) and equation (10) that:

$$D = D_z + D_\theta \quad (11)$$

For isotrope fractals equation (5) can be written even for ox and oy axes, and $D_x=D_y=D_z=D_0$. So:

$$N \sim N_x N_y N_z \sim r^{-(D_x + D_y + D_z)} = r^{-D}, \quad D = D_x + D_y + D_z = 3D_0 \quad (12)$$

Combining equations (11) and (12) the result is straightforward:

$$D = \frac{3D_\theta}{2} \quad (13)$$

where D_θ is the TEM micrograph fractal dimension, computed from gray-level distribution, using equation (9). It must be kept in mind that fractal behavior of the gray-level is assumed and "mass radius" relation is used to compute D_θ.

The above-considered theory is applied for computing fractal dimensions of some silica powders.

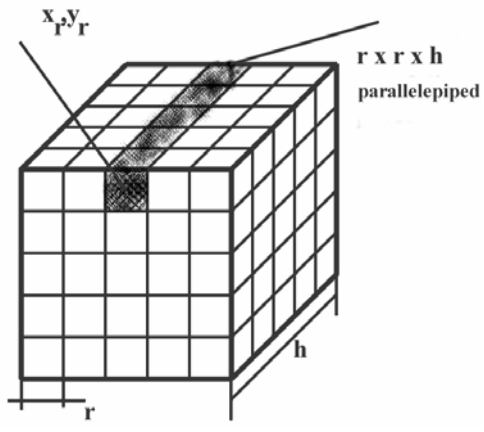

Fig. 1 – Grey parallelepiped r x r x h.

RESULTS AND DISCUSSION

Two samples of silica powders were analysed: sample **A** (figure 2), with BET surface area S=400m^2/g and sample **B** (figure 3) with BET surface area S=53m^2/g.

The powders had been produced in the Institute of Electronics, BAS by use of thermal arc plasma method. More about the powder synthesis can be found in literature.[15] Here only the major characteristics of the production will be discussed. Silica sand is used as raw material for ultrafine silica powder production. As the sand is a refractory material, the thermal arc plasma as very high enthalpy gas is a perfect circumstance for its vaporization. The vapor is cooled rapidly (10^5- 10^6 K/s) by mixing it with cooling gas in a flow reactor. The processes, carried out during the cooling, lead to production of ultrafine powders with different structures i.e. more or less aggregated.[15,16] Such powders can be analyzed from a fractal point of view to characterized their structure. So, it is interesting to determinate the powder fractal dimension.

From the TEM micrographs (Figure 2 and Figure 3), applying equations (9) and (11), fractal dimension of the images grey-levels are computed and using equation (13), fractal dimension of the 3-dimensional embedded object is obtained. Results from such calculations are presented in Figures 4 and 5.

These Figures show log-log plot of number of the occupied sites within R radius sphere for micrographs presented in Figures 2 and 3, respectively. TEM photo of figure 2 is a 725 pixels x 536 pixels image, 72 dpi and 3 pixels correspond to 7 nm. TEM photo of figure 3 is a 1105 pixels x 841 pixels image, 72 dpi. To compute fractal dimension we need to know the global behavior of the particles. This goal is achieved for TEM micrographs with low magnification.

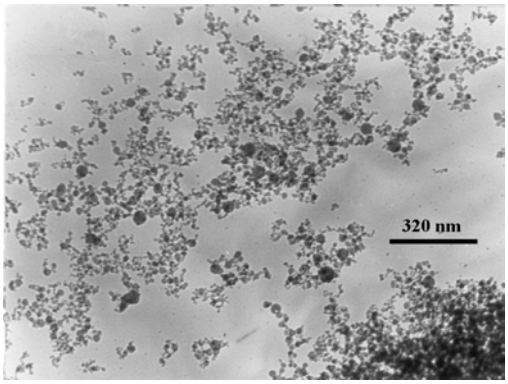

Fig. 2 – TEM micrograph of sample A.

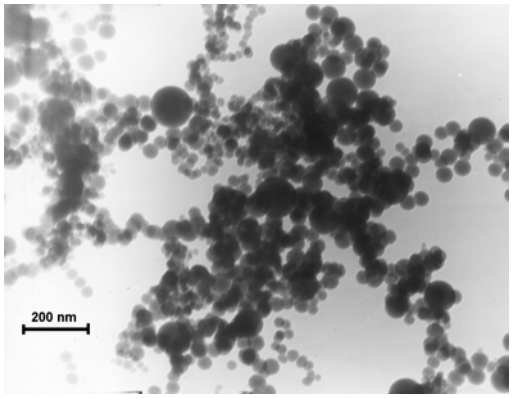

Fig. 3 – TEM micrograph of sample B.

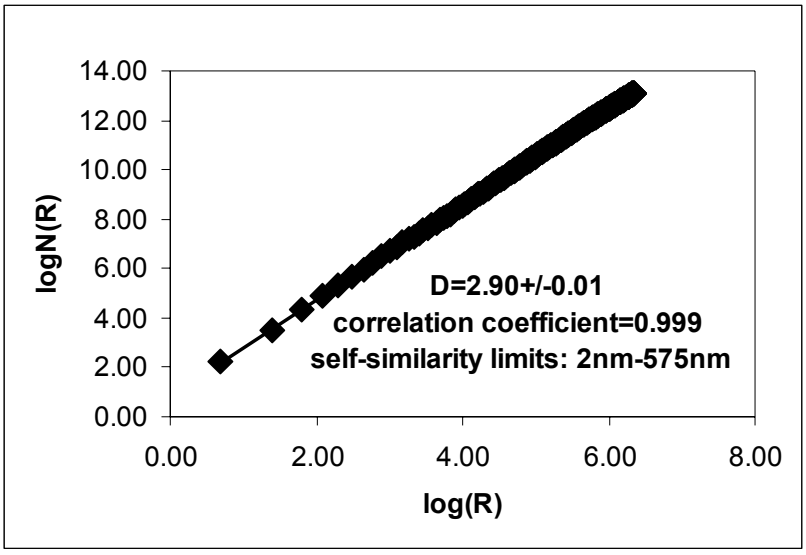

Fig. 4 – Log-log plot of number of occupied sites within R radius sphere for micrograph in Figure 2.

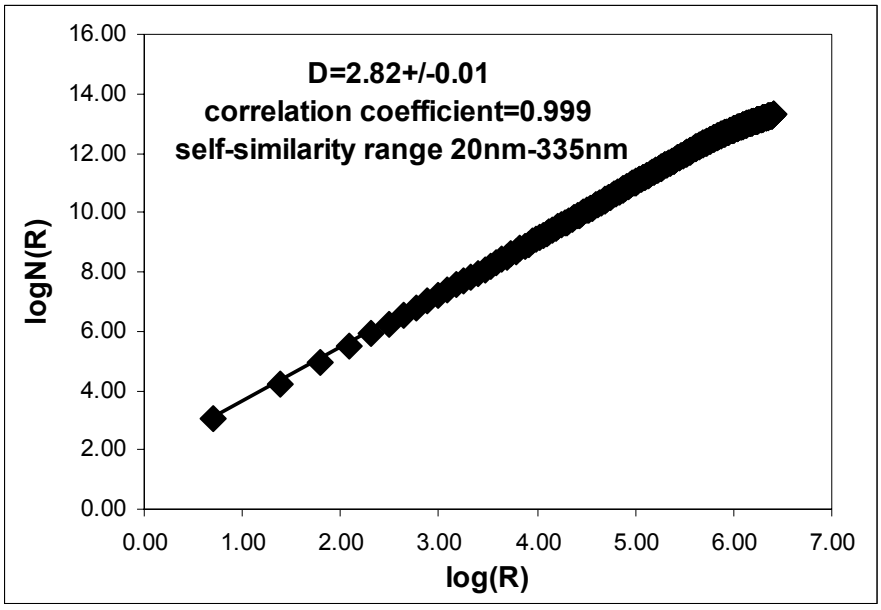

Fig. 5 – Log-log plot of number of occupied sites within R radius sphere for micrograph in Figure 3.

The obtained results show that both samples have a fractal behavior in a wide range and are characterized by a fractal dimension. The sample A has higher fractal dimension than that of the sample B.

This means that strong aggregation occurs at the sample A in the whole considered scale range 2nm-575 nm. Since the BET specific surface area of this sample is very high (400 g/m^2), i. e. the mean size of the particles is very small (7 nm), it can be expected that the aggregates will be formed by small individual particles. For the sample B two fractal dimension are calculated. The first one is 2.73±0.01 with correlation coefficient equal to 0.999. This fractal dimension is observed in the scale range 2nm-20nm. In the scale range 20nm-335 nm the calculated fractal dimension is 2.82±0.01 with correlation coefficient equal to 0.999.

The specific surface area is measured based on BET technique, that can access all of the "hidden" portions of the surface, undercuts, pores, etc. Some of these "hidden" portions may not be seen using TEM technique and measuring the surface height of each point (x,y).[17] The lower cut-off limit is 2 nm, indicating that beyond this limit we do not have any information in TEM technique, meanwhile as nitrogen molecule has a radius of, let say, 2 covalent nitrogen radius = 1.5 nm, the BET technique, using these molecules can "see", fine details, invisible in TEM images. This fact can be an explanation why meanwhile BET area varies from 400 m^2/g to 53 m^2/g , the fractal dimension varies just from 2.9 to 2.73 or 2.82.

Even in this situation the fractal dimension varies in the same way as the BET specific area.

To describe a surface, not only the fractal dimension is important, but the cut-off limits. Sample A is characterized by D=2.9 and a broad self-similarity domain (2nm-575nm) indicating a very rough surface.

Sample B has a lower fractal dimension and a narrow self-similarity domain showing a less rough surface.

The calculations show also that the samples are self-similar in the self-similarity limits. The property of self-similarity, that is the property for a part to look the same as the whole, is related to the preparation conditions. For both samples aggregation can occur but it will be higher at the sample A than at sample B because of its higher fractal dimension. The observed lowest fractal dimension at sample B (in the small scaling range 2nm-20 nm) can be explained by a correlation between points, situated at different depths, and separated in micrograph's plane by shorter distances.

CONCLUSIONS

A method for computing fractal dimensions from TEM micrographs was developed. This method was applied to ultrafine silica powders, produced by thermal arc plasma method. The investigated samples present good fractal structures with high fractal dimensions, between 2.8 and 2.9.

REFERENCES

1. B. B. Mandelbrot, “Fractals: Form, Chance and Dimension”, Freeman, San Francisco, 1977.
2. B. B. Mandelbrot, “The Fractal Geometry of Nature”, Freeman, San Francisco, 1982.
3. M. W. Mitchell and D. A. Bonnell, *J. Mat. Res.*, **1990**, *5*, 2244-2255 .
4. J. P. Carrejo, T. Thundat, L. A. Nagahara, S. M. Lindsay and A. Majumdar*, J.Vac. Sci. Technol B*, **1991**, *9*, 955-959.
5. D. R. Denley, *J.Vac. Sci. Technol A*, **1990,** *8*, 603-607.
6. J. M. Gomez-Rodriguez, A. M. Baro, L. Vasquez, R. C. Salvarezza, J. M. Vara and A. J. Arvia, *J. Phys. Chem,* **1992**, *96*, 347-350.
7. J. M. Williams and T. B. Beebe Jr., *J. Phys. Chem*, **1993**, *97*, 6249-6255; **1993**, *97*, 6255-6260.
8. J. J. Friel and C. S. Pande, *J. Mat. Res*, **1993**, *8*, 100-104.
9. G. Dobrescu, M. Crisan, M. Zaharescu, N. I. Ionescu, *Mater. Chem. Phys*, **2004**, *87*, 184-189.
10. D. I. dos Santos, M. A. Aegerter, A. F. Craievich, T. Lours and J. Zarzycki*, J. Non-Cryst. Solids*, **1987**, *95 & 96*, 1143-1150.
11. P. Pfeifer and M. Obert in “The Fractal Approach to Heterogeneous Chemistry” edited by D.Avnir, J.Wiley & Sons Ltd, 1989, p.11.
12. P. Grassberger, *Phys. Lett. A*, **1983**, *97*, 224-227.
13. P. Grassberger and I. Procaccia, *Physica* , **1983**, *9D*, 189-208.
14. J. Samios, P. Pfeifer, U. Mittag, M. Obert and T. Dorfmuler, *Chem. Phys. Lett*, **1986**, *128*, 545-550.
15. E. Balabanova and D. Oliver, "Factors influencing the aggregation of silica nanoparticles produced by thermal arc plasma method", in *Nanoscience&Nanotehnology'02 - Nanostructured materials application and innovation transfer*, edited by E. Balabanova, I. Dragieva, Heron Press Science Series 2002, p. 29-31.
16. E. Balabanova, *J. Opt. Adv. Mat,* **2003,** *5, 3*, 679-686.
17. J. Russ, “Fractal Surfaces”, Plenum Press, 1994, p. 62.